Journal of Sedimentary Research

Journal of Sedimentary Research, 2023, v. 93, 37–49 Research Article DOI: 10.2110/jsr.2022.044



GRAIN SIZE AND MINERAL VARIABILITY OF GLACIAL MARINE SEDIMENTS

JOHN T. ANDREWS, WENDY J. ROTH, AND ANNE E. JENNINGS²

Institute for Alpine and Arctic Research and Department of Geological Sciences, University of Colorado, Boulder, Colorado 80303, U.S.A.

Institute for Alpine and Arctic Research, University of Colorado, Boulder, Colorado 80303, U.S.A.

e-mail: andrewsj@colorado.edu

ABSTRACT: Glacial marine sediment deposition varies both spatially and temporally, but nearly all studies evaluate down-core (\sim time) variations in sediment variables with little consideration for across core variability, or even the consistency of a data set over distance scales of 1 to 1000 m. Grain size and quantitative X-ray diffraction (qXRD) methods require only \leq 1 g of sediment and thus analyses assume that the identification of coarse sand (i.e., ice-rafted debris) and sediment mineral composition are representative of the depth intervals. This assumption was tested for grain size and mineral weight % on core MD99-2317, off East Greenland. Samples were taken from two sections of the core that had contrasting coarse-sand content. A total of fourteen samples were taken consisting of seven (vertical) and two (horizontal) samples, with five replicates per sample for qXRD analyses and \sim 10 to 20 replicates for grain size. They had an average dry weight of 10.5 \pm 0.5 g and are compared with two previous sets of sediment samples that averaged 54.1 \pm 18.9 g and 20.77 \pm 5.8 g dry weight. The results indicated some significant differences between the pairs of samples for grain-size parameters (mean sortable silt, and median grain size) but little difference in the estimates of mineral weight percentages. Out of 84 paired mineral and grain-size comparisons only 17 were significantly different at p = < 0.05 in the *post-hoc* Scheffe test, all of which were linked to grain-size attributes.

INTRODUCTION

Glacial marine environments encompass a variety of sedimentary processes (turbid meltwater plumes, iceberg sediment rafting (Fig. 1), bottom-current transport, and resuspension by iceberg scouring) (Dowdeswell and Scourse 1990; Dowdeswell et al. 2000, 1994; Syvitski et al. 1996, 2001) that are probably not uniform over a region or even across the width of the typical core (10 cm). Sampling of marine cores invariably focuses on down-core changes of sediment or other properties (Ledbetter and Ellwood 1976) with the goal of reconstructing past changes in ocean climate or sediment transport and deposition (McCave and Andrews 2019a, 2019b).

An implicit assumption in nearly all studies is that the core is representative of the cored stratigraphic (e.g., seismic) unit, and multi-core or push cores (from a large box core) have usually not been investigated to confirm this assumption. Thus, the scale of lateral sediment variability in this environment (Fig. 1) is largely unknown, and not surprisingly little mention has been paid to possible variations across width intervals in cores. For example, the target population in this study is the Holocene sediment sequence in the small Grivel basin (~ 100 km²) located on the eastern Greenland shelf (Jennings et al. 2011), but the available population is only represented by core MD99-2317 (Fig. 2A). As the core's surface area is < 100 cm², this was but one of 10⁸/km² possible sites. A rarely noted assumption in paleo-marine studies is that the compositions (sediments, geochemical, biological) are representative of the target population. This is a reasonable assumption for several proxies, such as foraminifera (Perner et al. 2016), although their distribution can be patchy, but much less so for proxies linked to iceberg deposition, such as coarse grain sizes or mineralogy (Fig. 1). Thus, the basic question is how

representative of a specific ocean-glaciological setting is a single core and samples from that core?

Objectives

Lacking close adjacent cores from the area we resort to investigating the lateral (across core) variability in grain size and mineral sediment properties in paired samples from core MD99-2317 from the East Greenland continental shelf (Figs. 2, 3) using a between analysis-ofvariance (ANOVA) design and a post-hoc test for paired comparisons (Fig. 4). The questions that are addressed are: How variable are sediment properties between sample pairs from the same depth, and do the results suggest the need for more rigorous guidelines for sampling cores in these environments and even the acquisition of multiple cores? Differences might be expected between sample depth increments, but an implicit assumption is that the sample properties do not vary across the width of the core. In addition, the rate of sediment accumulation is certainly inherent in any considerations dealing with the representativeness of the selected samples. Because the measurements are replicated in this study, the data for both qXRD (Raven and Self 2017) and grain size are also an explicit evaluation of the precision of the methods.

CORE MD99-2317

Core MD99-2317 (henceforth #2317) was retrieved from Grivel Basin (Fig. 2A), a small basin on the East Greenland Shelf (68.103° N, 27.8615° W, 536 m wd, 25.07 m long), collected during the IMAGES V expedition (Labeyrie et al. 2003; Labeyrie and Jennings 2005). In most winters the landfast sea ice extends across the basin (Hastings 1960), which restricts

Published Online: January 2023

Copyright © 2023, SEPM (Society for Sedimentary Geology) 1527-1404/23/093-37





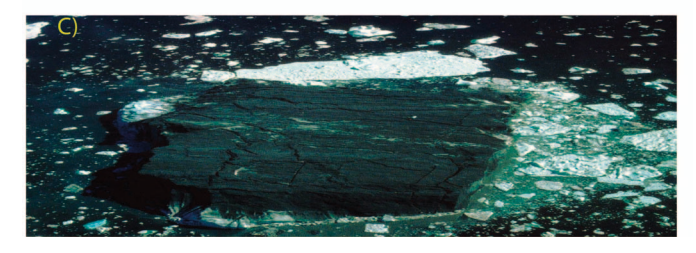


Fig. 1.—Photographs of icebergs showing: **A)** large iceberg off East Greenland ploughing through landfast sea ice, moving left to right (credit https://www.nasa.gov/mission_pages/icebridge/index.html.) **B)** Inclined debris bands in an iceberg. **C)** thick concentration of probable basalt-rich sediment from glacier traction zone near the MD99-2317 site. Melting and the release of sediment for deposition on the seafloor is spatially and temporally intermittent.

the movement of any embedded icebergs (Fig. 1A). Grivel Basin is only 30 to 40 km from a series of calving tidewater glaciers that flow across the Geikie Plateau, an extensive (60,000 km 2) early Tertiary basalt outcrop (Brooks 1990; Nuttall 1993) (Fig. 2A). Grivel Basin is also in the path of icebergs drifting south in the East Greenland Current (EGC) and sourced from large tidewater glaciers in Scoresby Sund and NE Greenland (Seale et al. 2011). The landfast sea ice breaks up in May to June, and heavy drifting sea ice is frequently present through July and September, with freeze-up starting in October (Hastings 1960). As an indication of the variability in iceberg and sea-ice concentrations Figure 2B illustrates the area immediately south of Grivel Basin.

Iceberg drift is mainly controlled by ocean currents, thus the vast majority of icebergs from East Greenland tidewater glaciers drift south along the East Greenland Shelf. Radar observations of iceberg numbers and their dimensions in September 1990 on the East Greenland Shelf (Dowdeswell et al. 1992, their Table 1) showed between 1 and 29, with widths of between 100 and 1000 m, and keel depths between 100 and 600 m. However, deep-drafted icebergs would be grounded on the shallow shelf that extends upstream from the Grivel Basin where the seafloor is heavily scoured (Syvitski et al. 2001). There is no historical data base for the yearly numbers of icebergs in the area, as there is for the Newfoundland Shelf (Bigg and Wilton 2014), although data from Iceland (1985–2011, Jonsdottir, *in* Andrews et al. 2019) documents changes in the number of icebergs observed on the NW/N Iceland shelf that are primarily linked to Scoresby Sund sources and transported in the East Iceland Current.

However, Fe-geochemical sediment data from MD99-2322, 160 km SW of #2317 (Darby et al. 2017) indicate that although the majority of the sand grains came from Scoresby Sund or NE Greenland, some grains had a signature from areas around the Arctic Ocean.

The sediment load in icebergs can be extremely variable (Bigg 2016) and depends on whether it includes the basal traction zone and subsequent transport and melt history (Dowdeswell and Scourse 1990) (Fig. 1). Sediment transport in this environment consists of sediment-rich meltwater plumes from the bases of tidewater glaciers (Syvitski et al. 1996; Mugford and Dowdeswell 2010; Mugford and Dowdeswell 2011) and transport of basal till carried away from the ice front in icebergs, which are often entrained in the frontal sikussuaq (Dwyer 1993, 1995) also referred to as a mélange of sea ice, icebergs, and bergy bits (Amundson et al. 2010). Iceberg drift in the area is restricted by the development of landfast sea ice (Hastings 1960), and many glaciers are fronted by a sikussuaq (Fig. 2B), which also delays iceberg movement onto the shelf and the reduction in iceberg sediment content. Typically, only a small fraction of the basal till (Fig. 1C) is made up of coarse sand, and the bulk of the sediment is of silt and clay size (Dreimanis and Vagners 1971; Dreimanis 1982). On this part of the East Greenland Shelf (Fig. 2), cold and fresh Polar Water overlies modified and chilled Atlantic Water (Jennings et al. 2011).

A depth–age model was constructed for #2317 based on 15 calibrated radiocarbon dates and the presence of the Vedde and Saksunarvatn tephras (Fig. 3A) (Jennings et al. 2006, 2011, 2014). The youngest radiocarbon date is at 312 cm, 86 cm from the core top at 226 cm, with an age of \sim 3200 cal yr BP. The sediment accumulation rates (SARs) for the section of the core included in this study (226 to 600 cm) varied from 25.6 to 10.6 yr/cm, potentially enabling multi-decadal to multi-century resolution of sediment records. Despite the closeness to glacial sources (Fig. 2A) the rate of sediment accumulation (SAR) at #2317 is < 1 mm/yr. These SARs can be compared with fjord to shelf estimates derived from studies just south of #2317 from Nansen to Kangerlussuaq fjords (Fig. 2) where SARs declined from 200–400 cm/ky in the fjords to < 10 cm/ky on the shelf (Andrews et al. 1994, their Fig. 7).

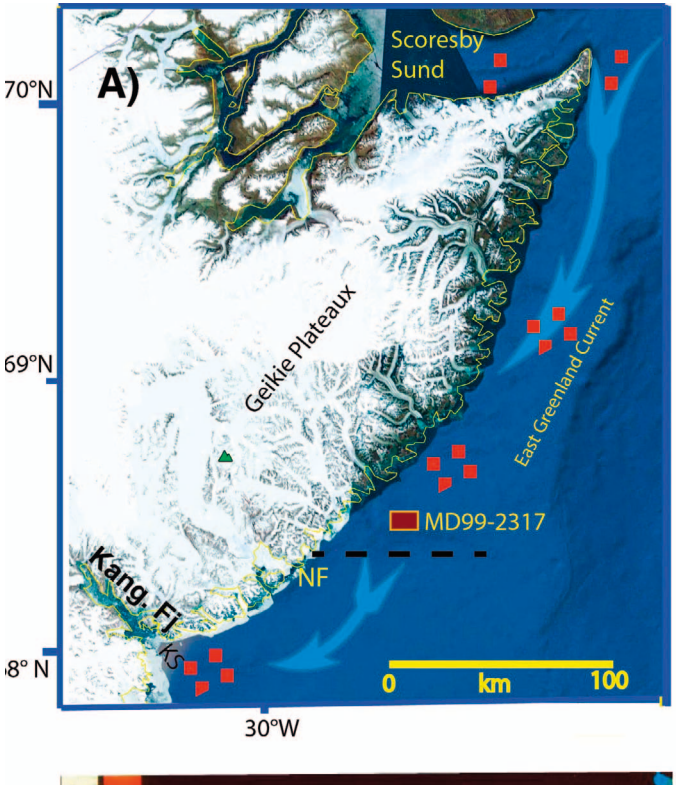
The rate of accumulation of iceberg rafted sediments is a function of: i) the sediment load and distribution in the icebergs (Fig. 1B, C), ii) the water temperatures, iii) the rate of wave erosion, and iv) the rate of iceberg drift (Fig. 1A) (Russel-Head 1980; Dowdeswell and Murray 1990; Venkatesh et al. 1994; Bigg 1999, 2016). Factors iii and iv suggest that deposition would be higher in the mainly ice-free summer months. Given our knowledge of the water-mass distribution on this part of the East Greenland Shelf (Jennings et al. 2011) it is probable that at Grivel Basin Irminger or Atlantic Intermediate waters ($> 1^{\circ}$ and $< 3^{\circ}$ C) extend beneath the Polar Water transported south in the East Greenland Current (Fig. 2A), and this would enhance melting of icebergs.

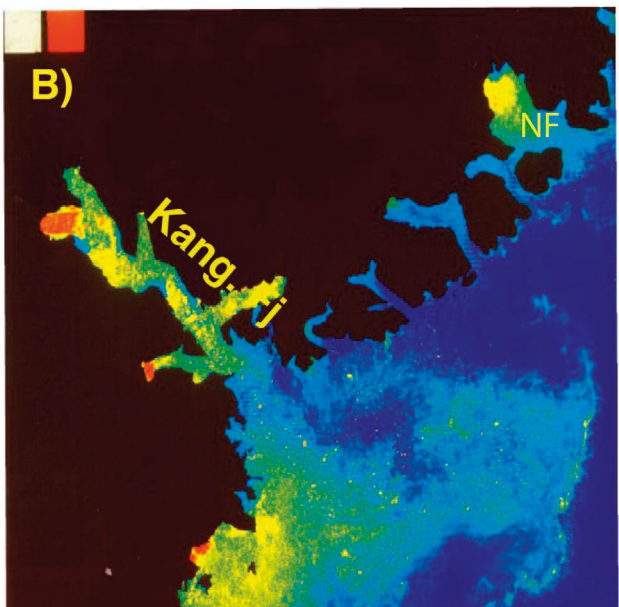
In the literature, ice-rafted debris (IRD) is often defined as various grain sizes > 63 μ m (Andrews 2000; McCave and Andrews 2019a) but it is important to note that silt- and clay-size sediments are also an integral result of glacial erosion (Dreimanis 1982). Our conceptual model for sediment deposition thus envisages the rapid settling of coarse sand from melting icebergs, whereas fine-grained sediments entrained in meltwater plumes or released from icebergs is transported by currents, with final composition determined by bottom-current flow speed (McCave and Andrews 2019a, their Fig. 1).

SEDIMENT VARIABILITY

Sampling and Methods

The on-board core description and subsequent examinations of the lithofacies of #2317 (Labreyrie et al. 2003, Leg 4, p. 644) indicate that "The uppermost unit (0–22 m) consists of a very dark gray silt clay, mostly homogeneous..." and the core logging of color and magnetic suscepti-





red = sikussuaq

yellow = heavy sea ice & icbergs

green = broken sea ice & open water

Light blue = light ice concentrations

Dark blue = open water

Fig. 2.—A) Location of the core site, MD99-2317, on the East Greenland Shelf (credit Google Earth). The cluster of small red squares are a schematic representation of iceberg transport along the shelf. B) False-color Landsat 1992 image of the area just south of the MD99-2317 site (Dwyer 1993, 1995), Kang Fj, Kangerlussuaq Fjord; NJ, Nansen Fjord. The heavy dashed line in Part A marks the northern limit of Part B.

bility confirmed this analysis. For this study the quality of the X-radiographs was such that we were unable to count IRD clasts > 2 mm (Grobe 1987) so inferences about iceberg rafting have been based on various sand fractions determined by either sieving or laser particle-size analysis (e.g., McKay et al. 2022). Previous research on #2317 included foraminifera and IRD history (Jennings et al. 2011), changes in mineral composition (Andrews et al. 2010), and evidence for changes in bottom-current flow speed (McCave and Andrews 2019a, 2019b) (Fig. 3A). The samples taken for foraminiferal studies had dimensions of ~ 8 cm \times 4 cm \times 2 cm, dry weights of 54.1 \pm 18.9 g, and a 2-cm sampling interval (n = 466) (Jennings et al. 2011). A second series (called here "GRL# samples") was undertaken combining sediment from two 10 cc plastic rings with

sample average dry weights of 20.77 ± 5.8 g (n = 100). For both these data sets, sand content was obtained by wet sieving through a > 63 μ m mesh and the volume wt% was obtained for the GRL# samples by using Malvern Mastersizer 3000 (see McKay et al. 2022). The GRL# samples were not always evenly spaced and the sampling of a rare event, such as the 23.1% sand (Table 1) in one sample, probably represents a restricted sediment avalanche from an iceberg such as shown in Figure 1C, and confirms the assumption that IRD records can be noisy.

Interpretations of geochemical and mineral and grain-size variations are also faced with the closed-array compositional conundrum (Chayes 1971; Templ et al. 2008) so that an increase in one size fraction necessitates a decrease in one or more other grain size bins resulting in spurious negative

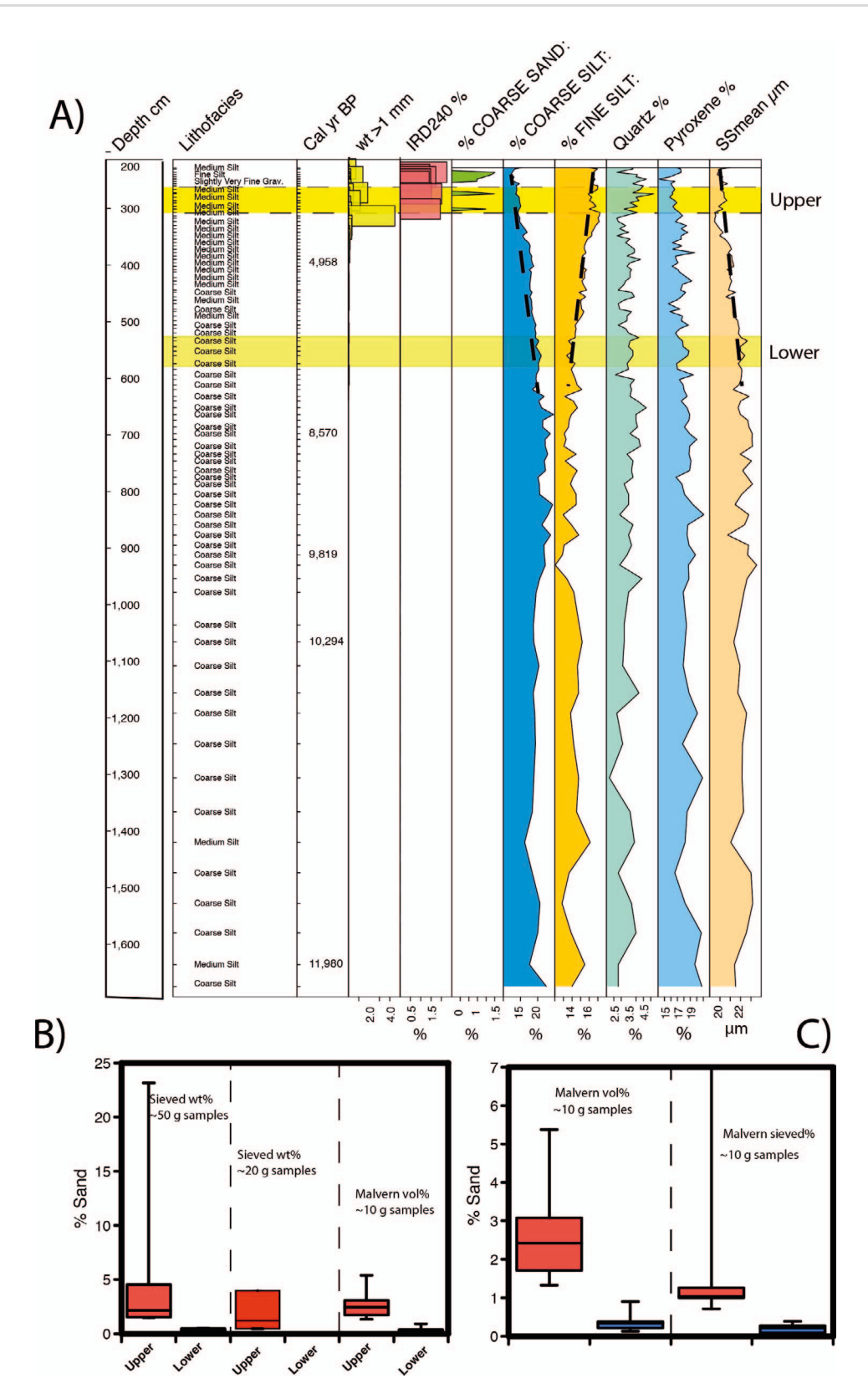


Fig. 3.—A) Downcore plot of MD99-2317 data showing sediment texture, some of the calibrated radiocarbon dates, grain-size parameters, and mineral weight %. The heavy dashed black lines show statistically significant trends in the data. The yellow rectangles highlight the two sections that are the focus of this study. B) Boxplots of the % of sand in the two sections (Upper and Lower) for the three sets of samples discussed in the text. C) Boxplots of the volume% and weight % of sand taken from the two sections of the core (Fig. 4).

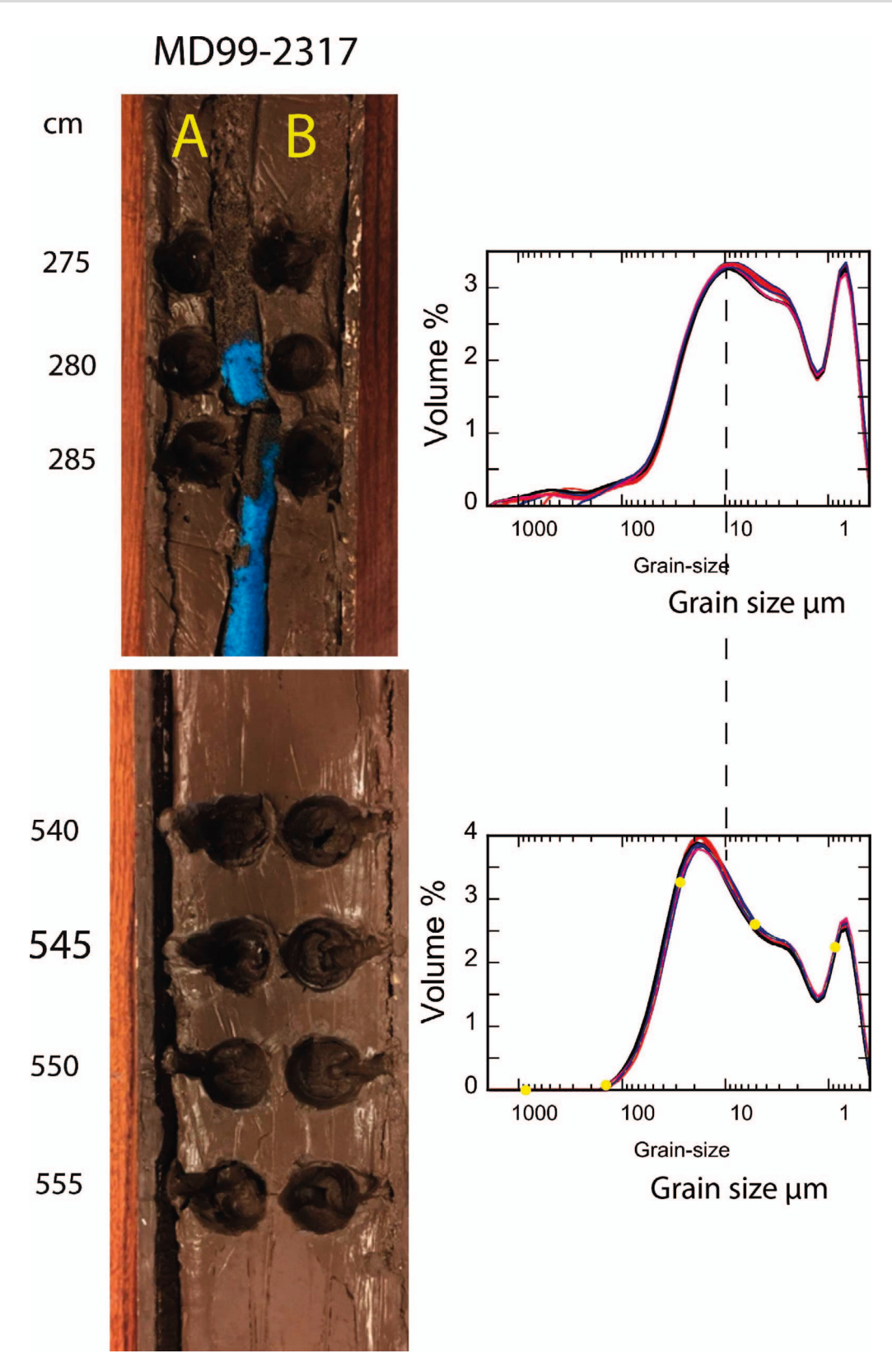


Fig. 4.—Photograph of the experimental A and B sampling for the two sections of MD99-2317and showing GRL# grain size distributions from samples in the two sections (see also Fig. 4) (n = 6 and 8 refer to the number of samples taken from the archive half of the core).

Table 1.—Comparison of the sample weights and sand estimates for the Upper and Lower sections (Fig. 4). A) Sampling for foraminifera, B) GRL# sampling for grain size and mineral composition and the Malvern sand fraction weight %s, C) initial sampling for this experiment, and D) the weight and percentages of sand in the 1 g sample.

	Mid-Depth,	Dry Sample Weight, g	> % 1000 μm	% Sand	Depth,	Initial Dry wt, g	% V Coarse Sand	Sand %	Depth	Dry Sediment Weight, g	% Sand	Dry Sediment Weight, g	% Sand
Upper	A)				B)				C)			D)	
	274	40.66	19.2	23.1	274	19.93	0.10	0.10	275A	9.77	0.67	1.0	1.71
	276	29.4747	3.2	4.5	280	15.58	0.00	0.00	275B	10.75	1.00	1.0	2.01
	278	37.81	0.4	1.5	286	17.39	0.00	0.00	279A	9.5	1.04	1.0	5.37
	280	33.707	0.3	1.6					279B	10.54	1.03	1.0	2.84
	282	37.808	0.9	2.2					285A	9.21	0.71	1.0	1.33
	284	35.291	3.3	4.5					285B	11.07	1.26	1.0	3.08
	286	40.326	0.6	1.5									
Lower	542	63.12	0.0	0.3	544	21.07	0.00	0.00	540A	10.6	0.03	1.0	0.35
	544	81.184	0.0	0.3	552	27.12	0.00	0.00	540B	10.44	0.10	1.0	0.9
	546	54.213	0.0	0.5	560	19.57	0.00	0.00	545A	10.81	0.07	1.0	0.24
	548	76.809	0.0	0.5					545B	10.95	0.24	1.0	0.33
	550	63.798	0.1	0.5					550A	11.36	0.39	1.0	0.41
	552	75.311	0.0	0.3					550B	9.99	0.25	1.0	0.35
	554	58.396	0.0	0.3					555A	11.47	0.19	1.0	0.13
	556	55.506	0.0	0.2					555B	11.23	0.30	1.0	0.18

correlations. No consistent data transformations have been implemented to address the issue, although Aitchison (1986) advocated the logratio transformation. However, in this paper we use the mineral and grain-size percentage data.

Samples from Lower (555–545 cm) and Upper (275–285 cm) sections (Figs. 3A, 4) were extracted for our experiment, the original data were taken from the working half of the core whereas the new samples were extracted from the archive-half (Fig. 4) (see Sampling Method, below). Seven depth intervals were sampled with two samples taken at each depth (Fig. 4; Table 1). All mineral and grain-size data presented is available electronically in the PANGAEA database (Andrews 2022). The sample volumes were ~ 10 cc and the dry weights averaged 10.55 \pm 0.64 g (Table 1). An extrapolated age for the section of the core ~ 280 cm (Fig. 3A) is ~ 2400 cal yr BP, whereas the calibrated age at ~ 550 cm is 7000 cal ka BP. Given the rates of sediment accumulation (Jennings et al. 2011) then the Lower 5-cm series are separated by ~ 60 yr versus 125 yr for the Upper sediments (Figs. 3A, 4).

Replicate qXRD data (see Sampling Method) were obtained from a 1 g split of the <2 mm sediment. Small sample statistics are defined as ≥ 5 (e.g., $0.5^5=0.03$) (Morgan 2017), which in our experiment called for a total of $7\times2\times5$ (n = 70) qXRD analyses. Sample recovery from the qXRD preparation resulted in a final sample weight usually between 0.5 and 0.8 g. As the XRD carousel holders hold ~ 0.25 g so our replicate five samples consisted of two splits and three re-runs.

Between-Sample ANOVA

The ANOVA null hypothesis, that parameter means are not significantly different between the paired samples (e.g., Fig. 4) (Dixon and Massey 1957; Davis 1986), is either accepted or rejected. If the null hypothesis is rejected a *post-hoc* test (NIST/SEMATECH 2012) is used to see which if any of the paired comparisons are significantly different. There are several *post-hoc* options available (Aabel 2016) and the selection depends of whether equal variances are assumed and/or equal replicate analyses are required. The Scheffe test is considered the most conservative for pairwise tests, but the Tukey-Kramer test is also appropriate (NIST/SEMATECH 2012). Equal variances are assumed but an equal number of samples is not required, ANOVA methods test derived parameters, such as the median

grain size or SS%, whereas Curray (Curray 1961) stressed the importance of the total grain-size spectra in understanding depositional processes. However, the problems inherent in particle size analysis (Fieller et al. 1992) restrict our ability to statistically compare the cumulative grain-size distributions.

RESULTS

qXRD Comparisons

The original 34 mineral wt% estimates are reduced by combining some of the minerals into larger groups, such as K-feldspar, plagioclase, and 1:1 and 2:1 clay minerals (Villaseñor and Jaeger 2014). For this paper the between-sample mineral variations for six minerals are compared (Table 2A), noting that embedded within the replicates is also machine variability (in this case a Siemens D5000 X-ray diffractometer). Five replicates of each sample were processed for a total of 7000 minutes of machine time. The boxplot (Fig. 5) gives a visual evaluation of the variations within a sample and between sample pairs (Fig. 4) however, we stress that we are dealing with comparisons between small samples, that is n=5 (Morgan 2017).

The actual mineral composition of our samples is not known, but the repeatability of the estimates is indicated by the standard deviations and the coefficient of variation (CV% a dimensionless number) (Table 2A). There is a voluminous literature on the application of CV% in statistics (Al-Jarallah and Aly 2014; Krishnamoorthy and Lee 2014) but here the results are simply reported. (Table 2A, B). The results indicate that 50% of the CV% statistic can be classified as very good (CV% < 10%) and 40% are good (CV% 10-20%) (Table 2). The remaining 10% are acceptable and were usually associated with disturbance during the automatic loading of the sample from the carousel. The between-sample ANOVA of the paired samples for the four non-clay and two clay minerals indicate that the null hypothesis of no difference was accepted except for quartz, pyroxene, and smectite (Table 3A; Fig. 5). Even in this case the post-hoc Scheffe indicated that no significant paired differences were detected. However, the problems associated with the qXRD data summing to 100% (Chayes 1971) are evident in the strong negative correlations between quartz and pyroxene and between pyroxene and smectite (-0.61 and -0.65), compared to 0.4 for the association between quartz and smectite.

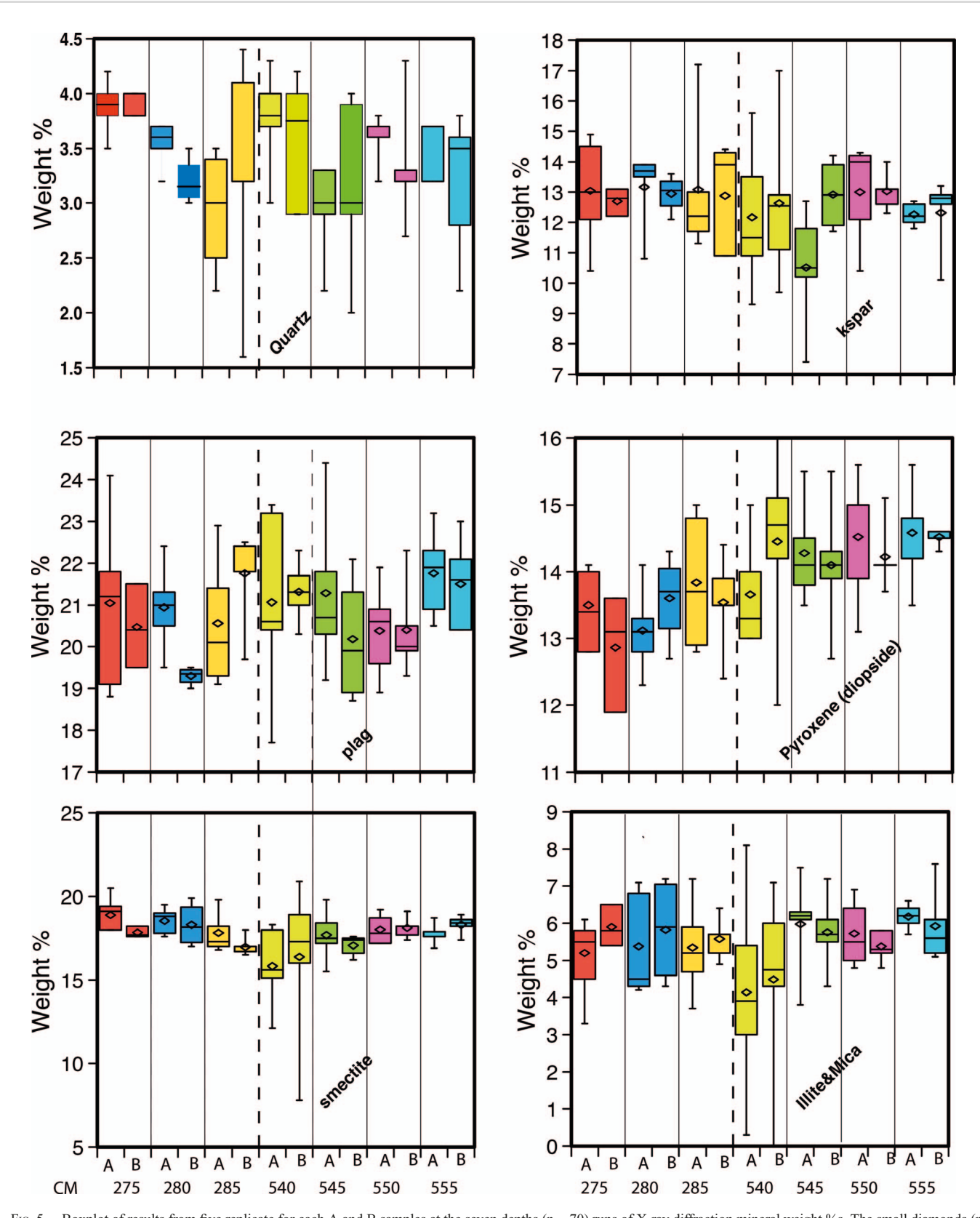


Fig. 5.—Boxplot of results from five replicate for each A and B samples at the seven depths (n = 70) runs of X-ray diffraction mineral weight %s. The small diamonds (not for quartz) are the mean values **A)** quartz wt%, **B)** K-feldspar, **C)** plag, plagioclase, **D)** pyroxene, **E)** smectite, **F)** illite and mica.

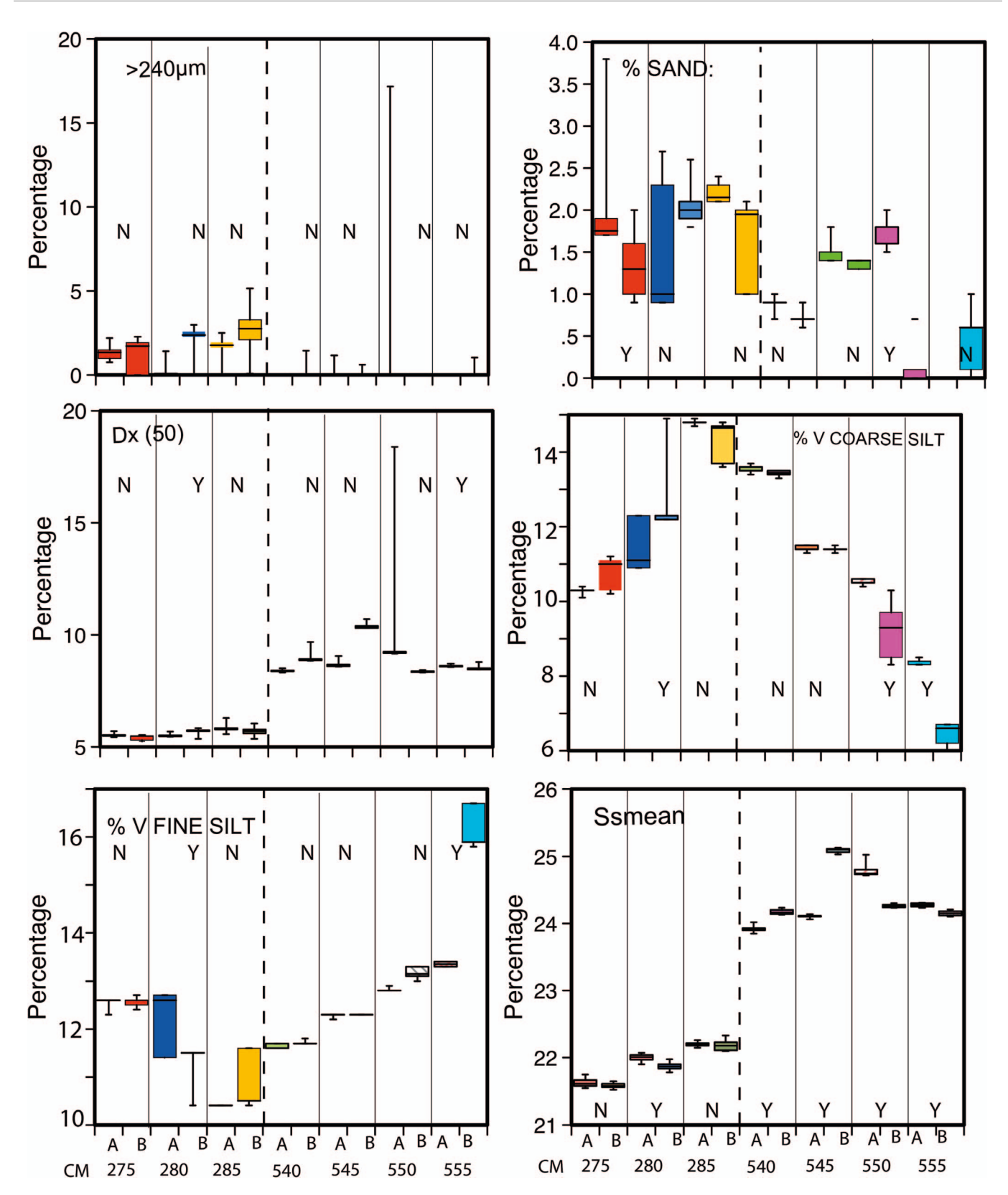


Fig. 6.—Boxplots of the paired samples (Fig. 5) for A) > 240 μ m, B) sand %, C) median grain-size μ m, D) very coarse silt %, E) very fine silt %, F) SS mean. The Y and N designations indicate whether the A versus B sample data are significantly different in the *post-hoc* Scheffe test.

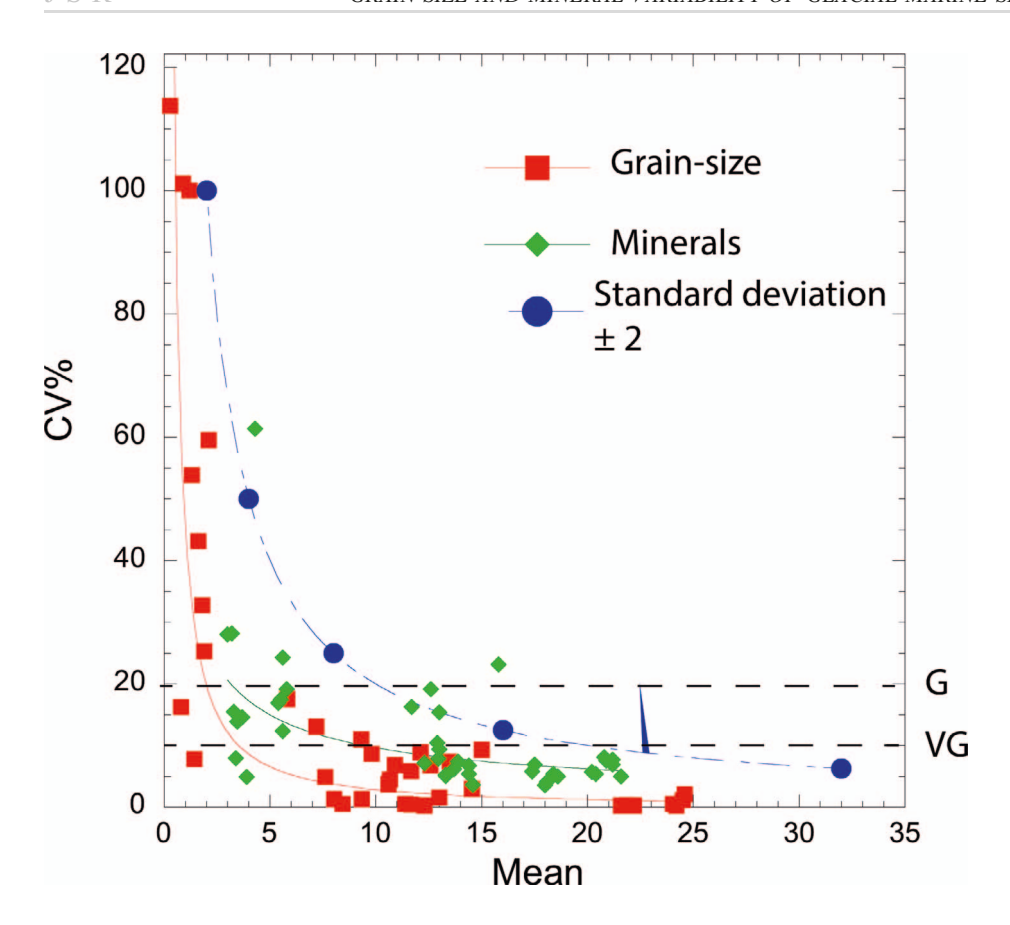


Fig. 7.—Plot of the means and CV% (Table 2) for the selected mineral (green) and grain-size variables (red) compared to a model (blue) with a fixed standard deviation of \pm 2 and varying means. The dashed horizontal dashed lines delimit CV% that are ranked good (G) or very good (VG).

The choice of a 5-cm depth interval (Fig. 4) was not a major factor in the experimental design, which was more concerned with variations across width intervals. The ANOVA on the depth increments (Table 3B) indicates significant differences in quartz, pyroxene, and smectite, but the *post-hoc* Scheffe test indicated no significant differences between the paired depth increments (Fig. 4), however the Tukey-Kramer *post-hoc* test indicates a single significant difference, and that is between pyroxene at 545 cm and 276 cm (Fig. 3A). ANOVA results on the Lower versus Upper sections also indicated significant differences in pyroxene (Figs. 3, 5; Table 3C).

Even though the data indicates that there are distinct trends for some minerals (Fig. 3A) the only clear changes are in pyroxene and smectite, both of which are associated with the glacial and periglacial erosion of the Greenland early Tertiary outcrop (e.g., Fig. 1B) (Andrews et al. 2015).

Grain Size

The two sections of the core have clear differences in their grain-size compositions with the ~550 cm samples having a major mode ~18 µm, whereas the ~280 cm samples have a broader and finer-grained peak (Fig. 4). There are also significant trends in at least some of the grain-size data (Fig. 3A, B). In an apparent contradiction both the fine silt and the coarse sand increase in the uppermost section (Fig. 3A), a reflection of both glacial plucking and abrasion (Boulton 1996; Andrews and Principato 2002; McCave and Andrews 2019a). Statistics for the grain-size variables are based on between 10 and 20 replicate runs (Table 2B). The absolute differences between paired cumulative A and B curves varies from 0.84% to 4,73% but there is no valid statistical test as to whether these differences are significant or not (Fieller et al. 1992).

The Gradistat program (Blott and Pye 2001) was used to reduce the 40 grain-size bins to seven descriptive categories as were the sortable silt parameters (McCave et al. 2017). The study focused on whether there are

differences in the A versus B pairs in terms of: i) $\% > 240 \mu m$, ii) % of sand (> 63 μm), iii) median grain size, iv) % very coarse silt, v) % very fine silt, and vi) the SS_{mean} (Fig. 6; Table 4).

It is not surprising that estimates of sand weight % versus volume %s vary (Fig. 3B) as the methods employ very different assumptions (Shillabeer et al. 1992, see also https://www.materials-talks.com/blog/201 7/06/13/laser-diffraction-vs-sieving-comparison/) and also are undertaken on very different sample weights (McKay et al. 2022). We compare sand content for samples from the Upper and Lower core intervals for the three data sets (Fig. 3A; Table 1), the results are portrayed as boxplots (Fig. 3B, C). All the comparisons indicate a significant difference between the Upper and Lower sections (Fig. 3A), reflecting an increase in ice rafting in the Upper section during Neoglaciation (Jennings et al. 2011). In the experimental data set (Fig. 4) the difference in sand % between the Upper sieved and volume wt%s is significant (p = 0.015), but the sand% estimates $(>63 \mu m)$ are not dissimilar for the Lower section percentages (Fig. 3C). Furthermore, sieving of the large $50 \pm g$ samples indicated a variable % of grains > 1000 µm in the Upper section and virtually none in the Lower (Table 1),

Plots of the average grain-size curves for the seven pairs of samples replicate the major differences in the grain-size curves for these two sections of the core, and reflect changes in regional sediment source-to-sink processes (Jennings et al. 2011; Perner et al. 2016). The box plot of the sediment variables (Fig. 6) suggests that whereas some pairs are similar others may have statistically different distributions. The null hypothesis is that there are no differences between the averages of the A versus B samples (Fig. 4); the *post-hoc* Scheffe was employed to test whether the paired samples were statistically similar and to avoid problems associated with the use of multiple t-tests. However, the Scheffe test (Fig. 5; Table 4A) indicates that out of the possible 42 paired comparisons (seven pairs and six variables) only 13 were significantly different (p = > 0.05). Of the six

Table 2.—A) qXRD mineral wt% estimates of the means, medians, standard deviations (n = 10), and the coefficient of variation (CV%). B) Grain size % estimates of the means, medians, standard deviations, and the coefficient of variation (CV%).

A) See Fig. (6						
Depth, cm	276	280	286	540	545	550	555
Quartz							
Mean:	3.9	3.4	3.2	3.7	3	3.46	3.3
Median:	3.9	3.5	3.3	3.85	3	3.45	3.55
Std. Dev.:	0.19	0.27	0.9	0.54	0.84	0.48	0.51
CV%	4.87	7.94	28.13	14.59	28.00	13.87	15.45
K-feldpsar	1.07	7.2	20.13	11.57	20.00	15.07	15.15
Mean:	12.9	12.95	13	12.6	11.7	13	12.3
Median:	12.9	13.5	12.6	12.6	11.7	13.1	12.5
Std. Dev.:	1.34	1.02	2	2.41	1.9	1.22	0.88
CV%	10.39	7.88	15.38	19.13	16.24	9.38	7.15
Plagioclase	10.59	7.00	13.36	19.13	10.24	9.30	7.13
8	20.0	20.2	21.2	21.2	20.0	20.4	21.6
Mean:	20.9	20.2	21.2	21.2	20.8	20.4	21.6
Median:	20.9	19.5	21.6	21.1	20.7	20.2	21.8
Std. Dev.:	1.57	1.15	1.46	1.63	1.68	1.09	1.08
CV%	7.51	5.69	6.89	7.69	8.08	5.34	5.00
Pyroxene							
Mean:	13.3	13.3	13.7	13.9	14.4	14.4	14.6
Median:	13.4	13.3	13.6	14.1	14.1	14.1	14.6
Std. Dev.:	0.69	0.67	0.85	1.03	0.97	0.77	0.53
CV%	5.19	5.04	6.20	7.41	6.74	5.35	3.63
Smecitite							
Mean:	18.6	18.4	17.4	15.8	17.5	18.1	18
Median:	18.2	18.8	17	16.3	17.5	18	18.1
Std. Dev.:	0.92	0.99	1.01	3.66	1.21	0.74	0.63
CV%	4.95	5.38	5.80	23.16	6.91	4.09	3.50
Illite and M	ica						
Mean:	5.4	5.6	5.5	4.3	5.8	5.6	6.1
Median:	5.7	4.9	5.5	4.4	6.1	5.4	6.1
Std. Dev.:	0.91	1.36	0.96	2.64	1.11	0.69	0.73
CV%	16.85	24.29	17.45	61.40	19.14	12.32	11.97
B) see Fig. 7		22	17.10	011.10	17.11	12.02	11.,,
Depth cm	276	280	286	540	545	550	555
		200	200	2.0	0.0	220	000
% > /40 H	n						
% > 240 μτ		30	20	20	20	20	25
N	25	30	20	20	20	20	25
N Mean:	25 1.3	1.2	2.1	0.13	0.11	0.86	0.11
N Mean: Median:	25 1.3 1.49	1.2 0.8	2.1 1.98	0.13 0	0.11 0	0.86 0	0.11 0
N Mean: Median: Std. Dev.:	25 1.3 1.49 0.7	1.2 0.8 1.2	2.1 1.98 1.25	0.13 0 0.39	0.11 0 0.3	0.86 0 3.8	0.11 0 0.37
N Mean: Median: Std. Dev.: CV%	25 1.3 1.49	1.2 0.8	2.1 1.98	0.13 0	0.11 0	0.86 0	0.11 0
N Mean: Median: Std. Dev.: CV% % > 63%	25 1.3 1.49 0.7 53.85	1.2 0.8 1.2 100.00	2.1 1.98 1.25 59.52	0.13 0 0.39 300.00	0.11 0 0.3 272.73	0.86 0 3.8 441.86	0.11 0 0.37 336.36
N Mean: Median: Std. Dev.: CV% % > 63% Mean:	25 1.3 1.49 0.7 53.85	1.2 0.8 1.2 100.00	2.1 1.98 1.25 59.52	0.13 0 0.39 300.00	0.11 0 0.3 272.73	0.86 0 3.8 441.86	0.11 0 0.37 336.36
N Mean: Median: Std. Dev.: CV% % > 63% Mean: Median:	25 1.3 1.49 0.7 53.85 1.6 1.6	1.2 0.8 1.2 100.00 1.8 1.95	2.1 1.98 1.25 59.52 1.9 2.1	0.13 0 0.39 300.00 0.8 0.9	0.11 0 0.3 272.73 1.42 1.4	0.86 0 3.8 441.86 0.88 1.1	0.11 0 0.37 336.36 0.29 0.1
N Mean: Median: Std. Dev.: CV% % > 63% Mean: Median: Std. Dev.:	25 1.3 1.49 0.7 53.85 1.6 0.69	1.2 0.8 1.2 100.00 1.8 1.95 0.59	2.1 1.98 1.25 59.52 1.9 2.1 0.48	0.13 0 0.39 300.00 0.8 0.9 0.13	0.11 0 0.3 272.73 1.42 1.4 0.11	0.86 0 3.8 441.86 0.88 1.1 0.89	0.11 0 0.37 336.36 0.29 0.1 0.33
N Mean: Median: Std. Dev.: CV% % > 63% Mean: Median: Std. Dev.: CV%	25 1.3 1.49 0.7 53.85 1.6 1.6	1.2 0.8 1.2 100.00 1.8 1.95	2.1 1.98 1.25 59.52 1.9 2.1	0.13 0 0.39 300.00 0.8 0.9	0.11 0 0.3 272.73 1.42 1.4	0.86 0 3.8 441.86 0.88 1.1	0.11 0 0.37 336.36 0.29 0.1
N Mean: Median: Std. Dev.: CV% % > 63% Mean: Median: Std. Dev.: CV% Median μm	25 1.3 1.49 0.7 53.85 1.6 1.6 0.69 43.13	1.2 0.8 1.2 100.00 1.8 1.95 0.59 32.78	2.1 1.98 1.25 59.52 1.9 2.1 0.48 25.26	0.13 0 0.39 300.00 0.8 0.9 0.13 16.25	0.11 0 0.3 272.73 1.42 1.4 0.11 7.75	0.86 0 3.8 441.86 0.88 1.1 0.89 101.14	0.11 0 0.37 336.36 0.29 0.1 0.33 113.79
N Mean: Median: Std. Dev.: CV% % > 63% Mean: Median: Std. Dev.: CV% Median μm Mean:	25 1.3 1.49 0.7 53.85 1.6 0.69 43.13	1.2 0.8 1.2 100.00 1.8 1.95 0.59 32.78	2.1 1.98 1.25 59.52 1.9 2.1 0.48 25.26	0.13 0 0.39 300.00 0.8 0.9 0.13 16.25	0.11 0 0.3 272.73 1.42 1.4 0.11 7.75	0.86 0 3.8 441.86 0.88 1.1 0.89 101.14 7.61	0.11 0 0.37 336.36 0.29 0.1 0.33 113.79 5.82
N Mean: Median: Std. Dev.: CV% % > 63% Mean: Median: Std. Dev.: CV% Median µm Mean: Median: Median:	25 1.3 1.49 0.7 53.85 1.6 0.69 43.13 8.02 7.98	1.2 0.8 1.2 100.00 1.8 1.95 0.59 32.78 9.32 9.56	2.1 1.98 1.25 59.52 1.9 2.1 0.48 25.26 10.89 11.25	0.13 0 0.39 300.00 0.8 0.9 0.13 16.25 9.35 9.35	0.11 0 0.3 272.73 1.42 1.4 0.11 7.75 8.42 8.41	0.86 0 3.8 441.86 0.88 1.1 0.89 101.14 7.61 7.75	0.11 0 0.37 336.36 0.29 0.1 0.33 113.79 5.82 5.12
N Mean: Median: Std. Dev.: CV% % > 63% Mean: Median: Std. Dev.: CV% Median Median: Median: Median: Median: Median:	25 1.3 1.49 0.7 53.85 1.6 1.6 0.69 43.13 8.02 7.98 0.1	1.2 0.8 1.2 100.00 1.8 1.95 0.59 32.78 9.32 9.56 1.02	2.1 1.98 1.25 59.52 1.9 2.1 0.48 25.26 10.89 11.25 0.74	0.13 0 0.39 300.00 0.8 0.9 0.13 16.25 9.35 9.35 0.12	0.11 0 0.3 272.73 1.42 1.4 0.11 7.75 8.42 8.41 0.04	0.86 0 3.8 441.86 0.88 1.1 0.89 101.14 7.61 7.75 0.37	0.11 0 0.37 336.36 0.29 0.1 0.33 113.79 5.82 5.12 1.02
N Mean: Median: Std. Dev.: CV% % > 63% Mean: Median: Std. Dev.: CV% Median μm Mean: Median: Std. Dev.: CV%	25 1.3 1.49 0.7 53.85 1.6 1.6 0.69 43.13 8.02 7.98 0.1 1.25	1.2 0.8 1.2 100.00 1.8 1.95 0.59 32.78 9.32 9.56	2.1 1.98 1.25 59.52 1.9 2.1 0.48 25.26 10.89 11.25	0.13 0 0.39 300.00 0.8 0.9 0.13 16.25 9.35 9.35	0.11 0 0.3 272.73 1.42 1.4 0.11 7.75 8.42 8.41	0.86 0 3.8 441.86 0.88 1.1 0.89 101.14 7.61 7.75	0.11 0 0.37 336.36 0.29 0.1 0.33 113.79 5.82 5.12
N Mean: Median: Std. Dev.: CV% % > 63% Mean: Median: Std. Dev.: CV% Median Median: Median: Median: Median: Median:	25 1.3 1.49 0.7 53.85 1.6 1.6 0.69 43.13 8.02 7.98 0.1 1.25	1.2 0.8 1.2 100.00 1.8 1.95 0.59 32.78 9.32 9.56 1.02	2.1 1.98 1.25 59.52 1.9 2.1 0.48 25.26 10.89 11.25 0.74	0.13 0 0.39 300.00 0.8 0.9 0.13 16.25 9.35 9.35 0.12	0.11 0 0.3 272.73 1.42 1.4 0.11 7.75 8.42 8.41 0.04	0.86 0 3.8 441.86 0.88 1.1 0.89 101.14 7.61 7.75 0.37	0.11 0 0.37 336.36 0.29 0.1 0.33 113.79 5.82 5.12 1.02
N Mean: Median: Std. Dev.: CV% % > 63% Mean: Median: Std. Dev.: CV% Median μm Mean: Median: Std. Dev.: CV%	25 1.3 1.49 0.7 53.85 1.6 1.6 0.69 43.13 8.02 7.98 0.1 1.25	1.2 0.8 1.2 100.00 1.8 1.95 0.59 32.78 9.32 9.56 1.02	2.1 1.98 1.25 59.52 1.9 2.1 0.48 25.26 10.89 11.25 0.74	0.13 0 0.39 300.00 0.8 0.9 0.13 16.25 9.35 9.35 0.12	0.11 0 0.3 272.73 1.42 1.4 0.11 7.75 8.42 8.41 0.04	0.86 0 3.8 441.86 0.88 1.1 0.89 101.14 7.61 7.75 0.37	0.11 0 0.37 336.36 0.29 0.1 0.33 113.79 5.82 5.12 1.02
N Mean: Median: Std. Dev.: CV% % > 63% Mean: Median: Std. Dev.: CV% Median μm Mean: Median: Std. Dev.: CV% V coarse sile	25 1.3 1.49 0.7 53.85 1.6 0.69 43.13 8.02 7.98 0.1 1.25	1.2 0.8 1.2 100.00 1.8 1.95 0.59 32.78 9.32 9.56 1.02 10.94	2.1 1.98 1.25 59.52 1.9 2.1 0.48 25.26 10.89 11.25 0.74 6.80	0.13 0 0.39 300.00 0.8 0.9 0.13 16.25 9.35 9.35 0.12 1.28	0.11 0 0.3 272.73 1.42 1.4 0.11 7.75 8.42 8.41 0.04 0.48	0.86 0 3.8 441.86 0.88 1.1 0.89 101.14 7.61 7.75 0.37 4.86	0.11 0 0.37 336.36 0.29 0.1 0.33 113.79 5.82 5.12 1.02 17.53
N Mean: Median: Std. Dev.: CV% % > 63% Mean: Median: Std. Dev.: CV% Median μm Mean: Median: Std. Dev.: CV% V coarse silt Mean:	25 1.3 1.49 0.7 53.85 1.6 1.6 0.69 43.13 8.02 7.98 0.1 1.25 t	1.2 0.8 1.2 100.00 1.8 1.95 0.59 32.78 9.32 9.56 1.02 10.94	2.1 1.98 1.25 59.52 1.9 2.1 0.48 25.26 10.89 11.25 0.74 6.80	0.13 0 0.39 300.00 0.8 0.9 0.13 16.25 9.35 9.35 0.12 1.28	0.11 0 0.3 272.73 1.42 1.4 0.11 7.75 8.42 8.41 0.04 0.48	0.86 0 3.8 441.86 0.88 1.1 0.89 101.14 7.61 7.75 0.37 4.86	0.11 0 0.37 336.36 0.29 0.1 0.33 113.79 5.82 5.12 1.02 17.53
N Mean: Median: Std. Dev.: CV% % > 63% Mean: Median: Std. Dev.: CV% Median μm Mean: Median: Std. Dev.: CV% V coarse silt Mean: Median:	25 1.3 1.49 0.7 53.85 1.6 1.6 0.69 43.13 8.02 7.98 0.1 1.25 t	1.2 0.8 1.2 100.00 1.8 1.95 0.59 32.78 9.32 9.56 1.02 10.94 12.1 12.2	2.1 1.98 1.25 59.52 1.9 2.1 0.48 25.26 10.89 11.25 0.74 6.80 14.55 14.8	0.13 0 0.39 300.00 0.8 0.9 0.13 16.25 9.35 9.35 0.12 1.28	0.11 0 0.3 272.73 1.42 1.4 0.11 7.75 8.42 8.41 0.04 0.48 11.4 11.4	0.86 0 3.8 441.86 0.88 1.1 0.89 101.14 7.61 7.75 0.37 4.86	0.11 0 0.37 336.36 0.29 0.1 0.33 113.79 5.82 5.12 1.02 17.53
N Mean: Median: Std. Dev.: CV% % > 63% Mean: Median: Std. Dev.: CV% Median μm Mean: Median: Std. Dev.: CV% V coarse silt Mean: Median: Std. Dev.:	25 1.3 1.49 0.7 53.85 1.6 0.69 43.13 8.02 7.98 0.1 1.25 t 10.6 10.1 0.39	1.2 0.8 1.2 100.00 1.8 1.95 0.59 32.78 9.32 9.56 1.02 10.94 12.1 12.2 1.08	2.1 1.98 1.25 59.52 1.9 2.1 0.48 25.26 10.89 11.25 0.74 6.80 14.55 14.8 0.44	0.13 0 0.39 300.00 0.8 0.9 0.13 16.25 9.35 0.12 1.28 13.5 13.5 0.99	0.11 0 0.3 272.73 1.42 1.4 0.11 7.75 8.42 8.41 0.04 0.48 11.4 11.4 0.06	0.86 0 3.8 441.86 0.88 1.1 0.89 101.14 7.61 7.75 0.37 4.86 9.8 10.35 0.85	0.11 0 0.37 336.36 0.29 0.1 0.33 113.79 5.82 5.12 1.02 17.53 7.2 6.7 0.94
N Mean: Median: Std. Dev.: CV% % > 63% Mean: Median: Std. Dev.: CV% Median μm Mean: Median: Std. Dev.: CV% V coarse silt Mean: Median: Std. Dev.: CV%	25 1.3 1.49 0.7 53.85 1.6 0.69 43.13 8.02 7.98 0.1 1.25 t 10.6 10.1 0.39	1.2 0.8 1.2 100.00 1.8 1.95 0.59 32.78 9.32 9.56 1.02 10.94 12.1 12.2 1.08	2.1 1.98 1.25 59.52 1.9 2.1 0.48 25.26 10.89 11.25 0.74 6.80 14.55 14.8 0.44	0.13 0 0.39 300.00 0.8 0.9 0.13 16.25 9.35 0.12 1.28 13.5 13.5 0.99	0.11 0 0.3 272.73 1.42 1.4 0.11 7.75 8.42 8.41 0.04 0.48 11.4 11.4 0.06	0.86 0 3.8 441.86 0.88 1.1 0.89 101.14 7.61 7.75 0.37 4.86 9.8 10.35 0.85	0.11 0 0.37 336.36 0.29 0.1 0.33 113.79 5.82 5.12 1.02 17.53 7.2 6.7 0.94
N Mean: Median: Std. Dev.: CV% % > 63% Mean: Median: Std. Dev.: CV% Median μm Median: Std. Dev.: CV% V coarse silt Mean: Median: Std. Dev.: CV% V fine silt	25 1.3 1.49 0.7 53.85 1.6 1.6 0.69 43.13 8.02 7.98 0.1 1.25 t 10.6 10.1 0.39 3.68	1.2 0.8 1.2 100.00 1.8 1.95 0.59 32.78 9.32 9.56 1.02 10.94 12.1 12.2 1.08 8.93	2.1 1.98 1.25 59.52 1.9 2.1 0.48 25.26 10.89 11.25 0.74 6.80 14.55 14.8 0.44 3.02	0.13 0 0.39 300.00 0.8 0.9 0.13 16.25 9.35 0.12 1.28 13.5 13.5 0.99 7.33	0.11 0 0.3 272.73 1.42 1.4 0.11 7.75 8.42 8.41 0.04 0.48 11.4 11.4 0.06 0.53	0.86 0 3.8 441.86 0.88 1.1 0.89 101.14 7.61 7.75 0.37 4.86 9.8 10.35 0.85 8.67	0.11 0 0.37 336.36 0.29 0.1 0.33 113.79 5.82 5.12 1.02 17.53 7.2 6.7 0.94 13.06
N Mean: Median: Std. Dev.: CV% % > 63% Mean: Median: Std. Dev.: CV% Median μm Median: Std. Dev.: CV% V coarse silt Mean: Median: Std. Dev.: CV% V fine silt Mean:	25 1.3 1.49 0.7 53.85 1.6 1.6 0.69 43.13 8.02 7.98 0.1 1.25 t 10.6 10.1 0.39 3.68	1.2 0.8 1.2 100.00 1.8 1.95 0.59 32.78 9.32 9.56 1.02 10.94 12.1 12.2 1.08 8.93 11.68	2.1 1.98 1.25 59.52 1.9 2.1 0.48 25.26 10.89 11.25 0.74 6.80 14.55 14.8 0.44 3.02	0.13 0 0.39 300.00 0.8 0.9 0.13 16.25 9.35 0.12 1.28 13.5 13.5 0.99 7.33	0.11 0 0.3 272.73 1.42 1.4 0.11 7.75 8.42 8.41 0.04 0.48 11.4 11.4 0.06 0.53	0.86 0 3.8 441.86 0.88 1.1 0.89 101.14 7.61 7.75 0.37 4.86 9.8 10.35 0.85 8.67	0.11 0 0.37 336.36 0.29 0.1 0.33 113.79 5.82 5.12 1.02 17.53 7.2 6.7 0.94 13.06
N Mean: Median: Std. Dev.: CV% % > 63% Mean: Median: Std. Dev.: CV% Median µm Mean: Median: Std. Dev.: CV% V coarse silt Mean: Median: Std. Dev.: CV% V fine silt Mean: Median:	25 1.3 1.49 0.7 53.85 1.6 1.6 0.69 43.13 8.02 7.98 0.1 1.25 t 10.6 10.1 0.39 3.68 12.57 12.6	1.2 0.8 1.2 100.00 1.8 1.95 0.59 32.78 9.32 9.56 1.02 10.94 12.1 12.2 1.08 8.93 11.68 12.6	2.1 1.98 1.25 59.52 1.9 2.1 0.48 25.26 10.89 11.25 0.74 6.80 14.55 14.8 0.44 3.02	0.13 0 0.39 300.00 0.8 0.9 0.13 16.25 9.35 0.12 1.28 13.5 13.5 0.99 7.33 11.68 11.7	0.11 0 0.3 272.73 1.42 1.4 0.11 7.75 8.42 8.41 0.04 0.48 11.4 11.4 0.06 0.53	0.86 0 3.8 441.86 0.88 1.1 0.89 101.14 7.61 7.75 0.37 4.86 9.8 10.35 0.85 8.67	0.11 0 0.37 336.36 0.29 0.1 0.33 113.79 5.82 5.12 1.02 17.53 7.2 6.7 0.94 13.06 15 15.9
N Mean: Median: Std. Dev.: CV% % > 63% Mean: Median: Std. Dev.: CV% Median µm Mean: Median: Std. Dev.: CV% V coarse silt Mean: Median: Median: Std. Dev.: CV% V fine silt Mean: Median: Std. Dev.: CV% V fine silt Mean: Median: Std. Dev.: CV% V fine silt Mean:	25 1.3 1.49 0.7 53.85 1.6 1.6 0.69 43.13 8.02 7.98 0.1 1.25 t 10.6 10.1 0.39 3.68 12.57 12.6 0.85	1.2 0.8 1.2 100.00 1.8 1.95 0.59 32.78 9.32 9.32 9.36 1.02 10.94 12.1 12.2 1.08 8.93 11.68 12.6 0.68	2.1 1.98 1.25 59.52 1.9 2.1 0.48 25.26 10.89 11.25 0.74 6.80 14.55 14.8 0.44 3.02	0.13 0 0.39 300.00 0.8 0.9 0.13 16.25 9.35 0.12 1.28 13.5 13.5 0.99 7.33 11.68 11.7 0.05	0.11 0 0.3 272.73 1.42 1.4 0.11 7.75 8.42 8.41 0.04 0.48 11.4 11.4 0.06 0.53 12.29 12.3 0.03	0.86 0 3.8 441.86 0.88 1.1 0.89 101.14 7.61 7.75 0.37 4.86 9.8 10.35 0.85 8.67	0.11 0 0.37 336.36 0.29 0.1 0.33 113.79 5.82 5.12 1.02 17.53 7.2 6.7 0.94 13.06 15 15.9 1.4
N Mean: Median: Std. Dev.: CV% % > 63% Mean: Median: Std. Dev.: CV% Median µm Mean: Median: Std. Dev.: CV% V coarse silt Mean: Median: Std. Dev.: CV% V fine silt Mean: Median: Std. Dev.: CV% Ssmean	25 1.3 1.49 0.7 53.85 1.6 1.6 0.69 43.13 8.02 7.98 0.1 1.25 t 10.6 10.1 0.39 3.68 12.57 12.6 0.85 6.76	1.2 0.8 1.2 100.00 1.8 1.95 0.59 32.78 9.32 9.56 1.02 10.94 12.1 12.2 1.08 8.93 11.68 12.6 0.68 5.82	2.1 1.98 1.25 59.52 1.9 2.1 0.48 25.26 10.89 11.25 0.74 6.80 14.55 14.8 0.44 3.02 10.66 10.4 0.48 4.50	0.13 0 0.39 300.00 0.8 0.9 0.13 16.25 9.35 9.35 0.12 1.28 13.5 13.5 0.99 7.33 11.68 11.7 0.05 0.43	0.11 0 0.3 272.73 1.42 1.4 0.11 7.75 8.42 8.41 0.04 0.48 11.4 11.4 0.06 0.53 12.29 12.3 0.03 0.24	0.86 0 3.8 441.86 0.88 1.1 0.89 101.14 7.61 7.75 0.37 4.86 9.8 10.35 0.85 8.67 13 12.95 0.2 1.54	0.11 0 0.37 336.36 0.29 0.1 0.33 113.79 5.82 5.12 1.02 17.53 7.2 6.7 0.94 13.06 15 15.9 1.4 9.33
N Mean: Median: Std. Dev.: CV% % > 63% Mean: Median: Std. Dev.: CV% Median µm Mean: Median: Std. Dev.: CV% V coarse silt Mean: Median: Std. Dev.: CV% V fine silt Mean: Median: Std. Dev.: CV% Ssmean Mean:	25 1.3 1.49 0.7 53.85 1.6 1.6 0.69 43.13 8.02 7.98 0.1 1.25 t 10.6 10.1 0.39 3.68 12.57 12.6 0.85 6.76	1.2 0.8 1.2 100.00 1.8 1.95 0.59 32.78 9.32 9.56 1.02 10.94 12.1 12.2 1.08 8.93 11.68 12.6 0.68 5.82 21.9	2.1 1.98 1.25 59.52 1.9 2.1 0.48 25.26 10.89 11.25 0.74 6.80 14.55 14.8 0.44 3.02 10.66 10.4 0.48 4.50	0.13 0 0.39 300.00 0.8 0.9 0.13 16.25 9.35 9.35 0.12 1.28 13.5 13.5 0.99 7.33 11.68 11.7 0.05 0.43 24.04	0.11 0 0.3 272.73 1.42 1.4 0.11 7.75 8.42 8.41 0.04 0.48 11.4 11.4 0.06 0.53 12.29 12.3 0.03 0.24 24.59	0.86 0 3.8 441.86 0.88 1.1 0.89 101.14 7.61 7.75 0.37 4.86 9.8 10.35 0.85 8.67 13 12.95 0.2 1.54	0.11 0 0.37 336.36 0.29 0.1 0.33 113.79 5.82 5.12 1.02 17.53 7.2 6.7 0.94 13.06 15 15.9 1.4 9.33 24.2
N Mean: Median: Std. Dev.: CV% % > 63% Mean: Median: Std. Dev.: CV% Median μm Mean: Median: Std. Dev.: CV% V coarse silt Mean: Median: Std. Dev.: CV% V fine silt Mean: Median: Std. Dev.: CV% Ssmean Mean: Median:	25 1.3 1.49 0.7 53.85 1.6 1.6 0.69 43.13 8.02 7.98 0.1 1.25 t 10.6 10.1 0.39 3.68 12.57 12.6 0.85 6.76 21.6 21.6	1.2 0.8 1.2 100.00 1.8 1.95 0.59 32.78 9.32 9.56 1.02 10.94 12.1 12.2 1.08 8.93 11.68 12.6 0.68 5.82 21.9 21.9	2.1 1.98 1.25 59.52 1.9 2.1 0.48 25.26 10.89 11.25 0.74 6.80 14.55 14.8 0.44 3.02 10.66 10.4 0.48 4.50 22.2 22.19	0.13 0 0.39 300.00 0.8 0.9 0.13 16.25 9.35 9.35 0.12 1.28 13.5 13.5 0.99 7.33 11.68 11.7 0.05 0.43 24.04 24.04 24.04	0.11 0 0.3 272.73 1.42 1.4 0.11 7.75 8.42 8.41 0.04 0.48 11.4 11.4 0.06 0.53 12.29 12.3 0.03 0.24 24.59 24.58	0.86 0 3.8 441.86 0.88 1.1 0.89 101.14 7.61 7.75 0.37 4.86 9.8 10.35 0.85 8.67 13 12.95 0.2 1.54 24.51 24.51	0.11 0 0.37 336.36 0.29 0.1 0.33 113.79 5.82 5.12 1.02 17.53 7.2 6.7 0.94 13.06 15 15.9 1.4 9.33 24.2 24.19
N Mean: Median: Std. Dev.: CV% % > 63% Mean: Median: Std. Dev.: CV% Median μm Mean: Median: Std. Dev.: CV% V coarse silt Mean: Median: Std. Dev.: CV% V fine silt Mean: Median: Std. Dev.: CV% Simean Mean: Median: Std. Dev.: CV%	25 1.3 1.49 0.7 53.85 1.6 1.6 0.69 43.13 8.02 7.98 0.1 1.25 t 10.6 10.1 0.39 3.68 12.57 12.6 0.85 6.76 21.6 21.6 0.05	1.2 0.8 1.2 100.00 1.8 1.95 0.59 32.78 9.32 9.56 1.02 10.94 12.1 12.2 1.08 8.93 11.68 12.6 0.68 5.82 21.9 0.079	2.1 1.98 1.25 59.52 1.9 2.1 0.48 25.26 10.89 11.25 0.74 6.80 14.55 14.8 0.44 3.02 10.66 10.4 0.48 4.50 22.2 22.19 0.058	0.13 0 0.39 300.00 0.8 0.9 0.13 16.25 9.35 9.35 0.12 1.28 13.5 13.5 0.99 7.33 11.68 11.7 0.05 0.43 24.04 24.04 24.07 0.13	0.11 0 0.3 272.73 1.42 1.4 0.11 7.75 8.42 8.41 0.04 0.48 11.4 11.4 0.06 0.53 12.29 12.3 0.03 0.24 24.59 24.58 0.508	0.86 0 3.8 441.86 0.88 1.1 0.89 101.14 7.61 7.75 0.37 4.86 9.8 10.35 0.85 8.67 13 12.95 0.2 1.54 24.51 24.5 0.27	0.11 0 0.37 336.36 0.29 0.1 0.33 113.79 5.82 5.12 1.02 17.53 7.2 6.7 0.94 13.06 15 15.9 1.4 9.33 24.2 24.19 0.068
N Mean: Median: Std. Dev.: CV% % > 63% Mean: Median: Std. Dev.: CV% Median μm Mean: Median: Std. Dev.: CV% V coarse silt Mean: Median: Std. Dev.: CV% V fine silt Mean: Median: Std. Dev.: CV% Ssmean Mean: Median:	25 1.3 1.49 0.7 53.85 1.6 1.6 0.69 43.13 8.02 7.98 0.1 1.25 t 10.6 10.1 0.39 3.68 12.57 12.6 0.85 6.76 21.6 21.6	1.2 0.8 1.2 100.00 1.8 1.95 0.59 32.78 9.32 9.56 1.02 10.94 12.1 12.2 1.08 8.93 11.68 12.6 0.68 5.82 21.9 21.9	2.1 1.98 1.25 59.52 1.9 2.1 0.48 25.26 10.89 11.25 0.74 6.80 14.55 14.8 0.44 3.02 10.66 10.4 0.48 4.50 22.2 22.19	0.13 0 0.39 300.00 0.8 0.9 0.13 16.25 9.35 9.35 0.12 1.28 13.5 13.5 0.99 7.33 11.68 11.7 0.05 0.43 24.04 24.04 24.04	0.11 0 0.3 272.73 1.42 1.4 0.11 7.75 8.42 8.41 0.04 0.48 11.4 11.4 0.06 0.53 12.29 12.3 0.03 0.24 24.59 24.58	0.86 0 3.8 441.86 0.88 1.1 0.89 101.14 7.61 7.75 0.37 4.86 9.8 10.35 0.85 8.67 13 12.95 0.2 1.54 24.51 24.51	0.11 0 0.37 336.36 0.29 0.1 0.33 113.79 5.82 5.12 1.02 17.53 7.2 6.7 0.94 13.06 15 15.9 1.4 9.33 24.2 24.19

grain-size variables that were used, the mean sortable silt difference indicated that five out of the seven paired samples (Fig. 6) were significantly different, whereas no differences were detected in the mean coarse sand percentages. However, the probability of having five significant differences out of seven comparisons is ~ 0.16 thus limiting any conclusive statement.

DISCUSSION

The results from this project raises a fundamental question as whether small sediment samples are representative of a 10-cm diameter core in an iceberg-rafting dominated region (Figs. 1, 2), and of course the core itself only samples a very small fraction of the target seismic sediment unit. The validity of conclusions drawn from the available (single core), to the much larger and unsampled target population, has been a fundamental problem in the Earth Sciences for several decades (Krumbein and Graybill 1965; Griffiths and Ondrick 1968), and this particularly applies to ice-proximal glacial marine environments where spatial variability in the deposited coarse IRD fraction is expected to occur. Iceberg deposition depends on melting and on the distribution of sediment in and on the iceberg, and this can result in spatially limited deposition (cm²) or a larger coverage (m²) if the iceberg becomes unstable and rolls (Fig. 1C). Only in the case of massive iceberg discharge, such as Hudson Strait Heinrich events, will coeval iceberg deposition take place over 10³ km² at 10³ yr scales (Hemming 2004; Andrews and Voelker 2018). Given the rates of sediment accumulation noted earlier, most sampling methods (Fig. 4) integrate decades to centuries of iceberg deposition and this plus bioturbation will tend to totally mask the cm- to µm-scale depositional, events that mark iceberg transport and sediment release (Fig. 1).

Working on Antarctica marine sediments, McKay et al. (2022) undertook a comprehensive analysis of methods used to identifying icerafted debris, namely X-radiography of > 2 mm clasts, the sieved wt% of sand > 250 μm , and the volumetric % of sand > 125 μm . One of their conclusions for the poor correlation between methods was "We suspect that the primary reason for this is the very small sample size(~ 0.15 –0.9 g) that is required for the correct obscuration of the laser particle sizer for samples of these lithologies." This conclusion supports our observations on #2317 and further calls for a consensus on what sediment fraction(s) can be termed "ice rafted" (Andrews 2000; McKay et al. 2022). In her informative commentary on the McKay et al. (2022) paper Cowan (2022) noted that the "...cleanest signal" of IRD is obtained by sieving out the > 250 µm coarse sand fraction. However, we add a caveat to that recommendation, sample weights should be as large as possible, understanding the usual constraints on core sample protocols. In addition, the nature of the bedrock and basal ice temperature has an influence on the amount of coarse debris produced during glacial erosion (Drewry 1986).

Analysis of the seven sets of paired data for mineral composition and grain-size attributes in general reveal that there is little statistical difference between the mineralogy of the paired samples, but there is more significant variability between the grain-size variables (Tables 3, 4; Figs. 5, 6). The CV% (Table 2A, B) is a commonly used measure of the repeatability of a measurement (Davis 1986). In the qXRD data, the CV% is usually < 20% (Table 2A) but varied from 3 to 61.4% (Fig. 7), but the overall conclusion is that the whole-pattern approach (Eberl 2003) to obtaining wt %s of mineral mixtures in marine sediment is robust (Raven and Self 2017). In terms of the grain-size data (Table 4), our results indicate that there can be considerable internal variability in the estimates of the > 240 and even the > 63 μ m fractions, whereas the replications for median grain size, % very coarse silt gave extremely small CV%s (Table 2) and that also applies to the calculations of SS_{mean}. How far this might be driven by changes in grain shape is an unknown (Marshall et al. 2014).

A plot of the mean and CV% data for the mineral wt%s and grain-size parameters (Fig. 7) indicates that they could be modeled by a power law,

TABLE 3.—A) ANOVA data for mineral variables (Fig. 5) showing the degree of freedom (df), the F statistic, probability of rejecting the null hypothesis (p), * = significant, and the number of significantly different paired comparison (# of 7), B) ANOVA results of between adjacent depths, C) ANOVA of the result of comparison between the upper versus lower sections (e.g., Figs. 3, 4).

				Scheffe Test	
Between A and B pairs	df	F	p	# of 7	
A)	13.56				
quartz		1.6	0.11		
K-feldspar		0.84	> 0.5		
plagioclase		1.08	0.396		
pyroxene		1.98	0.039*	0	
smectite		1.31	0.023*	0	
illite and mica		0.84	> 0.5		
B) Between depths	6.63				
quartz		2.44	0.035*		
K-feldspar		1.04	0.407		
plagioclase		1.13	0.351		
pyroxene		3.89	0.002*		
smectite		3.16	0.009*		
illite and mica		1.79	0.114		
C) Between U and L sections	1.68				
quartz		0.54	0.461		
K-feldspar		2.57	0.114		
plagioclase		0.431	> 0.5		
pyroxene		18.54	< 0.001*		
smectite		3.14	0.081		
illite and mica		0.028	> 0.5		

which suggests that the standard deviation is relatively constant regardless of the mean. However, there is a notable increase in the calculated CV% values for average values ≤ 3 .

Recommendations

The answers to the two primary questions that were raised are: Yes, there is some variability between paired samples (Figs. 5, 6; Tables 3, 4) and accordingly we argue that the sediment samples should be taken across the full breadth of the core to obtain the best representative sample for grain size and mineralogy. For example, an 8 cm \times 3 cm \times 0.5 cm sample would provide ~ 10 g dry weight of sediment, sufficient for several 1 g qXRD and grain size analyses and represents \sim 6 to 13 yr of accumulation in this study. The weight % of various sand fractions in this entire sample would be most representative indication of coarse IRD transport. Our results indicate that it is important to obtain as large a sample as possible if an objective is to define coarse IRD, given the usual constraints of sample sharing and multiple proxy requirements. For this purpose, the sieved weight % of the sand fractions is more representative than results obtained from the laser sizing of 1 g samples. Ideally a series of replicate 1 g samples will provide a sense of the mineral and grain-size variability (Tables 2-4), although we note that the qXRD and grain-size replicate measurements resulted in generally acceptable CV% estimates (Fig. 7).

CONCLUSION

In our focused study on glacial marine sediments in iceberg-dominated areas (Figs. 1, 2) some mineral and in particular some grain-size characteristics vary significantly across the same depth interval, and certainly between samples that are only 5 cm apart (Fig. 4). This does raise the larger question of the degree of spatial variability in sediment properties and the implicit assumption that "a core" is indeed

Table 4.—A) ANOVA data for grain-size variables (Fig. 6) showing the degree of freedom (df), the F statistic, probability of rejecting the null hypothesis (p), and the number of significantly different paired comparison (# of 7), B) ANOVA results of between adjacent depths, C) ANOVA of the result of comparison between the Upper versus Lower sections (e.g., Figs. 3, 4).

Between A and B pairs	df	F	p	# of 7
A)	13,146			
$% > 240 \; \mu m$		4.73	< 0.001	0
$% > 63 \mu m$		43.2	< 0.001	2
median μm		72.33	< 0.001	5
v. coarse silt		279.86	< 0.001	3
v. fine silt		258.14	< 0.001	2
SS mean		8313	< 0.001	5
B) Between depths	7,142			
$\% > 240~\mu m$		4.44	< 0.001	
$% > 63 \mu m$		28.88	< 0.001	
median μm		110.63	< 0.001	
v. coarse silt		225.34	< 0.001	
v. fine silt		86.25	< 0.001	
SS mean		748.28	< 0.001	
C) Between U and L sections	1,158			
$\% > 240 \; \mu m$		22.87	< 0.001	
$% > 63 \mu m$		101.87	< 0.001	
median μm		52.78	< 0.001	
v. coarse silt		33.96	< 0.001	
v. fine silt		49.35	< 0.001	
SS mean		2448.9	< 0.001	

representative of the region's depositional history. This assumption is rarely, if ever, tested, and grain-size variability in these regions is aptly shown by the change in wt% of sand between 274 and 278 cm (Table 1). The data support the initial concern that estimates of the sand fraction, especially the coarse fraction, can be underrepresented in grain-size methods that require a sample size of 1 g or less, a conclusion also reached by McKay et al. (2022) based on a detailed study of Antarctic core samples. Estimates of the weight % or volume % of sand are dependent on the methods used and on the mass of sediment available for study. Even in areas close to calving tidewater glaciers (Figs. 1, 2) the amount of coarse sand > 250 μm is not large, and this suggests that the small samples (≤ 1 g) taken for laser-sizer grain-size methods (Syvitski 1991) may not always be representative of the coarse IRD fraction (Table 1A), but we also note that the bulk of sediments produced by glacial erosion is $< 63 \mu m$ (Dreimanis 1976, 1982). This suggests that paleoceanographers also need to use provenance tools to document glacially derived sediments (Licht and Hemming 2017).

The glacial marine environment that we have described here is not radically different from other areas of the world with tidewater glaciers, and our concerns about spatial sampling have wide application. However, to understand the full range of variability of glacial marine sediment, multiple cores from the same basin need to be studied, but this is an unlikely scenario.

SUPPLEMENTAL MATERIAL

Sample Preparation for the Malvern Master Sizer 3000 and Quantitative X-Ray Diffraction is available from the SEPM Data Archive: https://www.sepm.org/supplemental-materials. The full mineral and grain-size data are archived in the Pangaea data base (Andrews 2022; www.Pangaea.de). The submitted material also includes the full grain-size data for MD99-2317 (see McCave and Andrews 2019a, 2019b).

ACKNOWLEDGMENTS

We acknowledge the support of National Science Foundation grant #1804504. Core MD99-2317 was obtained with the support of National Science Foundation grant OCE-98-09001 and with the assistance of the crew and researchers on the *Marion Dufresne*. We appreciate the comments of Dr. Jaia Syvitski on a draft of this manuscript. We acknowledge the suggestions and comments of Dr. Tania Villaseñor, Dr. Jean-Carlos Montero-Serrano, and an anonymous reviewer which have resulted in improvements to the initial submission. John Southard provided much needed grammar and reference editing on the final draft.

REFERENCES

- AABEL, 2016, Aabel NG software package, www.gigawiz.com/.
- AITCHISON, J., 1986, The Statistical Analysis of Compositional Data: London, Chapman and Hall, 416 p.
- AL-JARALLAH, R., AND ALY, E.-E.A.A., 2014, Nonparametric Tests for comparing several coefficients of variation: Communications in Statistics, Theory and Methods, v. 43, p. 3602–3613
- AMUNDSON, J.M., FAHNESTOCK, M., TRUFFER, M., BROWN, J., LUTHI, M.P., AND MOTYKA, R.J., 2010, Ice melange dynamics and implications for terminus stability, Jakobshavn Isbrae Greenland: Journal of Geophysical Research, Earth Surface, v. 115.
- Andrews, J.T., 2000, Icebergs and iceberg rafted detritus (IRD) in the North Atlantic: facts and assumptions: Oceanography, v. 13, p. 100–108.
- Andrews, J.T., 2022, Mineral and grain size data for sediment core MD99-2317. PANGAEA, doi:10.1594/PANGAEA.940546.
- ANDREWS, J.T., AND PRINCIPATO, S.M., 2002, Grain-size characteristics and provenance of ice-proximal glacial marine sediments (or why do grain-size analyses anyway?), in Dowdeswell, J.A., and O'Cofaigh, C., eds., Glacier-Influenced Sedimentation at High-Latitude Continental Margins: Geological Society of London, Special Publication 203, p. 305–324.
- Andrews, J.T., Voelker, A., 2018, "Heinrich events" (& sediments): a history of terminology and recommendations for future usage: Quaternary Science Reviews, v. 187, p. 31–40.
- Andrews, J.T., Milliman, J.D., Jennings, A.E., Rynes, N., Dwyer, J., 1994, Sediment thicknesses and Holocene glacial marine sedimentation rates in three east Greenland Fjords (ca. 68°N): Journal of Geology, v. 102, p. 669–683.
- Andrews, J.T., Bjork, A.A., Eberl, D.D., Jennings, A.E., and Verplanck, E.P., 2015, Significant differences in late Quaternary bedrock erosion and transportation: East versus West Greenland $\sim 70^{\circ}$ N and the evolution of glacial landscapes: Journal of Quaternary Science, v. 30, p. 452–463.
- Andrews, J.T., Jónsdóttir, I., and Geirsdóttir, A., 2019, Tracking Holocene drift-ice limits on the NW/SW Iceland shelf: comparing proxy data with observation and historical evidence: Arctic, Antarctic, and Alpine Research, v. 51, p. 96–114.
- Bigg, G.R., 1999, An estimate of the flux of iceberg calving from Greenland: Arctic, Antarctic, and Alpine Research, v. 31, p. 174–178.
- Bigg, G.R., 2016, Icebergs: Their Science and Links to Global Change: Cambridge University Press, 240 p.
- BIGG, G.R., AND WILTON, D.J., 2014, Iceberg risk in the Titanic year of 1912: was it exceptional?: Weather, v. 69, p. 100–104.
- BLOTT, S.J., AND PYE, K., 2001, GRADISTAT: a grain size distribution and statistics package for the analysis of unconsolidated sediments: Earth Surface Processes and Landforms, v. 26, p. 1237–1248.
- BOULTON, G.S., 1996, Theory of glacial erosion, transport and deposition as a consequence of subglacial sediment deformation: Journal of Glaciology, v. 42, p. 43–62.
- Brooks, C.K., 1990, Kangerdlugssuaq Studies: Processes at a Rifted Continental Margin: University of Copenhagen, Geological Institute,100 p.
- CHAYES, F., 1971, Ratio correlation: Chicago, University of Chicago Press, 99 p.
- Cowan, E.A., 2022, Unraveling the deep-sea sedimentary record of ice sheet history: Paleoceanography and Paleoclimatology, v. 37, p. 1–4.
- Curray, J.R., 1961, Tracing sediment masses by grainsize modes: 21st International Geological Congress, Cophenhagen, p. 119–130.
- DARBY, D.A., ANDREWS, J.T., BELT, S.T., JENNINGS, A.E., AND CABEDO-SANZ, P., 2017, Holocene cyclic records of ice-rafted debris and sea ice variations on the East Greenland and NW Iceland margins: Antarctic, Arctic, and Alpine Research, v. 49, p. 649–672.
- DAVIS, J.C., 1986, Statistics and Data Analysis in Geology: New York, John Wiley & Sons, 646 p.
- DIXON, W.J., AND MASSEY, F.J.J., 1957, Introduction to Statistical Analysis: New York, McGraw-Hill Book Company, 488 p.
- DOWDESWELL, J.A., AND MURRAY, T., 1990, Modelling rates of sedimentation from icebergs, in Dowdeswell, J.A., and Scourse, J.D., eds., Glacimarine Environments: Processes and Sediments: Geology Society of London, Special Publication 53, p. 121–137.
- Dowdeswell, J.A., and Scourse, J.D., 1990, Glacimarine Environments: Processes and Sediments, *in* Dowdeswell, J.A., and Scourse, J.D., eds., Glacimarine Environments: Geological Society of London, Special Publication 53, p. 155–176.

- Dowdeswell, J.A., Whittington, R.J., and Marienfeld, P., 1994, The origin of massive diamicton facies by iceberg rafting and scouring, Scorsby Sund, East Greenland: Sedimentology, v. 41, p. 21–35.
- Dowdeswell, J.A., Whittington, R.J., Jennings, A.E., Andrews, J.T., Mackensen, A., and Marinfeld, P., 2000, An origin for laminated glacimarine sediments through sea-ice build-up and supressed iceberg rafting: Sedimentology, v. 47, p. 557–576.
- DREIMANIS, A., 1976, Tills: their origin and properties, in Legget, R.F., ed., Glacial Till an Inter-Disciplinary Study: The Royal Society of Canada, Special Publication 12, p. 11– 40
- Dreimanis, A., 1982, Genetic classification of Tills and Criteria for their Differentiation: Progress Report on Activities 1977–1982, and definitions of glacigenic terms, INQUA: Commission on Genesis and Lithology of Quaternary Deposits, Report on Activities 1977–1982
- DREIMANIS, A., AND VAGNERS, U.J., 1971, Bimodel distribution of rock and mineral fragments in basal tills, in Goldthwaite, R.P., ed., Till: A Symposium: Ohio State University Press, p. 237–250.
- Drewry, D., 1986, Glacial Geologic Processes: London, Edward Arnold, 270 p.
- DWYER, J.L., 1993, Monitoring characteristics of glaciation in the Kangerdlugssuaq Fjord region, East Greenland, using digital LANDSAT MSS and TM Data [MSDC Thesis]: University of Colorado, Boulder, 202 p.
- DWYER, J.L., 1995, Mapping tide-water glacier dynamics in East Greenland using Landsat data: Journal of Glaciology, v. 41, p. 584–596.
- EBERL, D.D., 2003, User guide to RockJock: a program for determining quantitative mineralogy from X-ray diffraction data: U.S. Geological Survey, Open-File Report 03-78, 40 p.
- FIELLER, N.R.J., FLENLEY, E.C., AND OLBRICHT, W., 1992, Statistics of particle-size data: Royal Statistical Society, Series C, Applied Statistics, Journal, v. 41, p. 127–146.
- Grobe, H., 1987, A simple method for the determination of ice-rafted debris in sediment cores: Polarforschung, v. 57, p. 123–126.
- HASTINGS, A.D., 1960, Environment of Southeast Greenland: U.S. Army, Quatermaster Research and Engineering Command, 62 p.
- HEMMING, S.R., 2004, Heinrich Events: massive late Pleistocene detritus layers of the North Atlantic and their global climate imprint: Reviews of Geophysics, v. 42, RG1005/2004.
- JENNINGS, A.E., HALD, M., SMITH, L.M., AND ANDREWS, J.T., 2006, Freshwater forcing from the Greenland Ice Sheet during the Younger Dryas: evidence from southeastern Greenland shelf cores: Quaternary Science Reviews, v. 25, p. 282–298.
- JENNINGS, A.E., ANDREWS, J.T., AND WILSON, L., 2011, Holocene environmental evolution of th SE Greenland Shelt north and south of the Denmark Strait: Irminger and East Greenland current interactions: Quaternary Science Reviews, v. 30, p. 980–998.
- JENNINGS, A.E., THORDARSON, T., ZALZAL, K., STONER, J.F., HAYWARD, C., GEIRSDOTTIR, A., AND MILLER, G.H., 2014, Holocene tephra from Iceland and Alaska Record in SE Greenland Shelf sediments, in Austin, W.E.N., Abbott, P.M., Davis, S.M., Pearce, N.J.G., and Wastegard, S., eds., Marine Tephrachronology: Royal Society of London, Special Publication 398, p. 157–193.
- Krishnamoorthy, K., and Lee, M., 2014, Improved tests for the equality of normal coefficients of variation: Computational Statistics, v. 29, p. 215–232.
- LABEYRIE, L.D., AND JENNINGS, A.E., 2005, Physical properties of sediment core MD99-2323, doi:10.1594/PANGAEA.256517.
- LABEYRIE, L., JANSEN, E., AND CORTIJO, E., 2003, Les rapports de campagnes a la mer MD114/IMAGES V: Brest, Institut Polaire Français Paul-Emile Victor.
- Ledbetter, M.T., and Ellwood, B.B., 1976, Selection of sample intervals in deep-sea sedimentary cores: Geology, v. 4, p. 303–304.
- LICHT, K.J., AND HEMMING, S.R., 2017, Analysis of Antarctic glacigenic sediment provenance through geochemical and petrologic applications: Quaternary Science Reviews, v. 164, p. 1–24.
- MARSHALL, N.R., PIPER, D.J.W., SAINT-ANGE, F., AND CAMPBELL, D.C., 2014, Late Quaternary history of contourite drifts and variations in Labrador Current flow, Flemish Pass, offshore eastern Canada: Geo-Marine Letters, v. 34, p. 457–470.
- McCave, I.N., and Andrews, J.T., 2019a, Distinguishing current effects in sediments delivered to the ocean by ice. I. Principles, methods and examples: Quaternary Science Reviews, v. 212, p. 92–107.
- McCave, I.N., Andrews, J.T., 2019b, Distinguishing current effects in sediments delivered to the ocean by ice. II. Glacial to Holocene changes in North Atlantic high latitude upper ocean flows: Quaternary Science Reviews, v. 223, no. 105902.
- McCave, I.N., Thornalley, D.J.R., and Hall, I.R., 2017, Relation of sortable silt grain size to deep-sea current speeds: calibration of the "Mud Current Meter": Deep-Sea Research, Part I, Oceanographic Research Papers, v. 127, p. 1–12.
- McKay, R., Albot, O., Dunbar, G.B., Lee, J.I., Lee, M.K., and Yoo, K.-C., et al., 2022, A comparison of methods for identifying and quantifying ice rafted debris on the Antarctic margin: Paleoceanography and Paleoclimatology, v. 37, doi:10.1029/2021PA004404.
- MORGAN, C.J., 2017, Use of proper statistical techniques for research studies with small samples: American Journal of Physiology, Lung Cellular and Molecular Physiology, v. 313, p. 873–877.
- MUGFORD, R.I., AND DOWDESWELL, J.A., 2010, Modeling iceberg-rafted sedimentation in high-latitude fjord environments: Journal of Geophysical Research, Earth Surface, v. 115, 21 p., F03024, doi:10.1029/2009JF001564, 2010.
- MUGFORD, R.I., AND DOWDESWELL, J.A., 2011, Modeling glacial meltwater plume dynamics and sedimentation in high-latitude fjords: Journal of Geophysical Research, Earth Surface, v. 116, F01023, doi:10.1029/2010jf001735.

- NIST/SEMATECH, 2012, E-Handbook of Statistical Methods, http://www.itl.nist.gov/div898/handbook/.
- NUTTALL, A.-M., 1993, Glaciological Investigations in East Greenland using Digital LANDSAT imagery [M.Phil. Thesis]: Cambridge, 107 p.
- Perner, K., Jennings, A.E., Moros, M., Andrews, J.T., and Wacker, L., 2016, Interaction between warm Atlantic-sourced waters and the East Greenland Current in northern Denmark Strait (68°N) during the last 10,600 cal a BP: Journal of Quaternary Science, v. 31, p. 472–483.
- RAVEN, M.D., AND SELF, P.G., 2017, Outcomes of 12 years of the Reynolds Cup quantitative mineral analysis round robin: Clays and Clay Minerals, v. 65, p. 122–134.
- Russel-Head, D.S., 1980, The melting of free-drifting icebergs: Annals of Glaciology, v. 1, p. 119–122.
- SEALE, A., CHRISTOFFERSEN, P., MUGFORD, R.I., AND O'LEARY, M., 2011, Ocean forcing of the Greenland Ice Sheet: calving fronts and patterns of retreat identified by automatic satellite monitoring of eastern outlet glaciers: Journal of Geophysical Research, Earth Surface, v. 116, 16 p.
- SHILLABEER, N., HART, B., AND RIDDLE, A.M., 1992, The use of a mathematical-model to compare particle-size data derived by dry-sieving and laser analysis: Estuarine Coastal and Shelf Science, v. 35, p. 105–111.

- SYVITSKI, J.P.M., 1991, Principles, Methods, and Applications of Particle Size Analysis: London, Cambridge University Press, 368 p.
- SYVITSKI, J.P.M., ANDREWS, J.T., AND DOWDESWELL, J.A., 1996, Sediment deposition in an iceberg-dominated glacimarine environment, East Greenland: basin fill implications: Global and Planetary Change, v. 12, p. 251–270.
- SYVITSKI, J.P.M., STEIN, A., ANDREWS, J.T., AND MILLIMAN, J.D., 2001, Icebergs and seafloor of the East Greenland (Kangerlussuaq) continental margin: Arctic, Antarctic and Alpine Research, v. 33, p. 52–61.
- TEMPL, M., FILZMOSER, P., AND REIMANN, C., 2008, Cluster analysis applied to regional geochemical data: problems and possibilities: Applied Geochemistry, v. 23, p. 2198– 2213.
- Venkatesh, S., Murphy, D.L., and Wright, G.F., 1994, On the deterioration of icebergs in the marginal ice-zone: Atmosphere-Ocean, v. 32, p. 469–484.
- VILLASEÑOR, T., AND JAEGER, J.M., 2014, Data report: quantitative powder X-ray diffraction analysis from the Canterbury Basin, Expedition 317: International Ocean Drilling Program, Proceedings, v. 317, p. 1–38.

Received 17 May 2022; accepted 22 October 2022.